CHEMISTRY
AN ASIAN JOURNAL

DOI: 10.1002/asia.200700013

PAMAM Dendrimers as Anchors for the Preparation of Electrocatalytically Active Ultrathin Metallic Films

Subash C. Raghu, Sheela Berchmans,* Kanala L. Phani, and Venkatraman Yegnaraman[a]

Abstract: This paper describes the formation of catalytically active thin films of Pt, Pt/Au, and Pt/Ru on gold substrates stabilized by amine-terminated polyamidoamine (PAMAM) dendrimers. A monolayer of dendrimer is initially self-assembled on the gold substrate, which serves as a template for the growth of catalytically active thin films. As dendrimers contain tens to hundreds of functional groups at the periphery, the aggregate strength of the multidentate interactions with the gold substrate leads to the formation of robust films. The films were found to exhibit high catalytic activity for the oxidation of small hydrocarbons such as methanol. Such films offer versatility and scope for the design of effective electrocatalysts, especially in the context of microfuel cells and "dendrichips"; hence, they could find applications in the fields of sensors, fuel cells, and waste-water treatment.

Keywords: cyclic voltammetry · dendrimers · electrocatalysis · electrochemistry · heterogeneous catalysis

Introduction

Dendrimers are highly branched, three-dimensional macromolecules with well-defined structures constructed around a central core.[1–4] Their special architecture arises due to their extraordinary symmetry, high branching, and maximized terminal functionality density. This architecture has led to a number of applications for dendrimer molecules, such as agents in resonance imaging, catalysts, gene vectors, photon transduction, antioxidants, antimicrobial agents, and so on.[5–7] Incorporation of nanoparticles onto electrode surfaces to realize electrocatalysis has always been a fascinating and challenging study. Direct deposition of nanoparticles leads to unstable and non-adherent films on electrode surfaces. The basic requirement for a stable, adherent film with maximum coverage is a matrix on the electrode surface that holds the nanoparticles intact, prevents their agglomeration, allows free diffusion of electroactive species to the nanoparticles, and provides an electrical link between the substrate and the nanoparticles. Conducting polymer film is a suitable choice for the matrix in terms of holding nanoparticles, but it impedes the free diffusion of electroactive species to the nanoparticles trapped deep in the film. Alternatively, metal nanoparticles can be linked to the electrode by employing self-assembled monolayers (SAMs) of suitable molecules as spacers. However, it was observed that the electrical communication between the dendrimer-encapsulated metal nanoparticles linked through an SAM and the electrode surface is not as fast as expected.[8] Many researchers have prepared dendrimer–metal nanocomposites, which are based on metal complexation by the tertiary amine groups present inside the dendrimer followed by chemical reduction with borohydride. Metals such as Pt, Pd, Au, and Ag can be coordinated within the dendrimers, and the dendrimer-encapsulated nanoparticles can be nearly monodispersed; even though the latter are passive towards aggregation, enough of the surface is accessible for them to be catalytically active.[9–15] The preparation of bimetallic dendrimer-encapsulated nanoparticles and their catalysis have recently been reported, as well as the presence of a cooperative effect attributed to the presence of bimetallic particles.[16–19]

In almost all cases of catalytic reactions of dendrimer-encapsulated nanoparticles reported, only chemical catalysis of hydrogenation and the Heck coupling reaction have been carried out to a large extent. There are only two reports that discuss the electrocatalysis of oxygen reduction with dendrimer-encapsulated nanoparticles.[20,21] The hydroxy-terminated dendrimers, which were either physically adsorbed onto gold substrates or linked to the glassy carbon electrodes through oxidative coupling, were tested to be electroca-

[a] S. C. Raghu, Dr. S. Berchmans, Dr. K. L. Phani, Dr. V. Yegnaraman
Central Electrochemical Research Institute
Karaikudi 630006, Tamil Nadu (India)
Fax: (+91) 4565-227-779
E-mail: sheelaberchmans@yahoo.com

Supporting information for this article is available on the WWW under http://www.chemasianj.org or from the author.

talytically active towards oxygen reduction. In this approach, linking of dendrimer-encapsulated nanoparticles without loss of their electrocatalytic activity on the electrode surface posed problems. As dendrimers are polar molecules, they assume an open structure; consequently, the catalytic nanoparticles tend to leach out from the electrode surface. It was observed that depending on the polarity of the solvents, the dendrimer structure becomes either closed or open, and this structure variation is responsible for the loss of the electrocatalytic effect. Polyamidoamine (PAMAM) dendrimers of generations 3.5 and 5.5 have been used to prepare dendrimer-encapsulated nanoparticles of Au and bimetallic Au/Ag.[22,23] Au–dendrimer nanocomposites were shown to exhibit antioxidant properties, and the bimetallic Au/Ag nanoparticles were shown to catalyze the reduction of *p*-nitrophenol. We recently showed that dendrimer (PAMAM 4.5)-encapsulated Pt nanoparticles chemically linked to gold substrates through a cystamine monolayer exhibited electrocatalytic activity towards the oxidation of small molecules such as methanol, ethanol, and ethylene glycol.[8] In a recent study,[24] we showed that a fourth-generation amine-terminated PAMAM dendrimer aids the formation of nanoparticulate thin films of platinum on gold. In this paper, we make use of the self-assembly of fourth-generation amine-terminated PAMAM dendrimers ($G4NH_2$) on gold substrates as an anchor layer for the growth of platinum films, which exhibited very good catalytic activity. A base layer of dendrimer was initially self-assembled on the gold substrate, over which Pt was chemically reduced by controlled heating under reflux in the presence of hydroxylamine hydrochloride. Dendrimers, by virtue of their branched nature with numerous tertiary amine groups, enable the fixing of the metal particles and at the same time allow the facile diffusion of electroactive species deep into the film. We prepared electrocatalytically active thin films of Pt, Pt/Au, and Pt/Ru with $G4NH_2$ as anchor layers on gold substrates. As dendrimers contain tens to hundreds of functional groups at the periphery, the aggregate strength of the multidentate interactions with the gold substrate leads to the formation of robust films. The electrocatalytic behavior of the films towards the oxidation of small molecules such as methanol is also discussed herein.

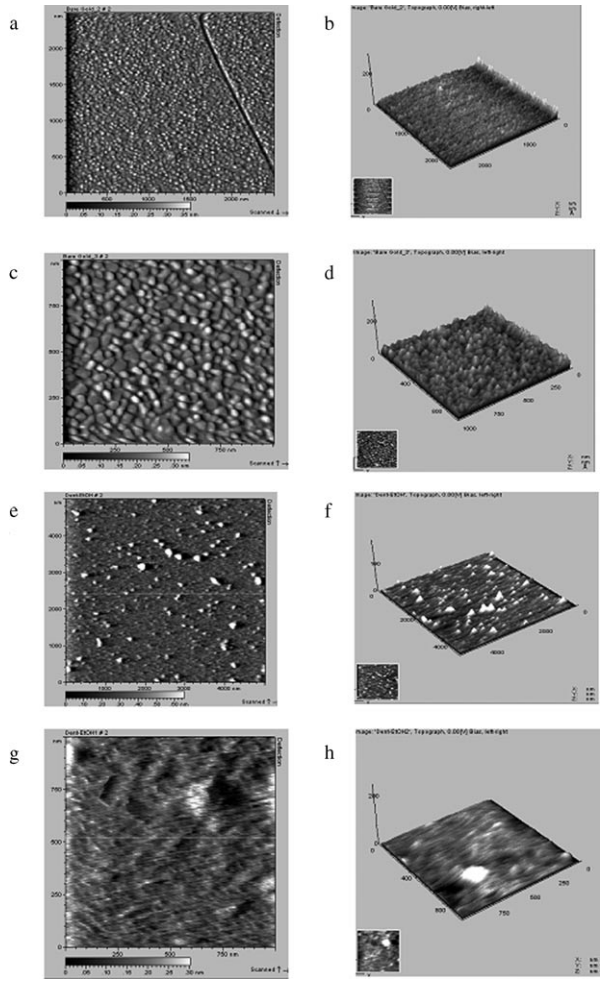

Figure 1. AFM images showing the topography of a–d) the bare gold substrate and e–h) the dendrimer-modified gold substrate. b, d, f, and h) Three-dimensional view. Areas of substrate under view are 5×5 μm^2 (a and e) and 1×1 μm^2 (c and g).

Results and Discussion

Figure 1a–d shows the AFM images of the gold substrate used in this work. Figure 1e–h depicts the surface of the gold substrate modified by the fourth-generation amine-terminated dendrimer; the topography of the dendrimer film self-assembled on the gold substrate is clearly visible. Figure 1f and h represents the three-dimensional view of the film. The average height of the film is 4–6 nm. This clearly shows that the dendrimer forms a monolayer on the gold substrate. The molecular size of the dendrimer molecule used in this work is 4.5 nm. The formation of the dendrimer film can also be explicitly seen on comparison with Figure 1a–d, which depicts the topography of the bare gold substrate. Figure 1a and b shows the gold substrate over an area of 5×5 μm^2. Figure 1c and d shows the gold substrate over an area of 1×1 μm^2. Similarly, Figure 1e and f and Figure 1g and h correspond to an area of 5×5 and 1×1 μm^2, respectively. The morphological characteristics of the film are clearly seen in the figure. When seen over a large area (Figure 1e), the film characteristics are not very clear. In Figure 1g, the dendrimer film appears like a woven mat. The formation of the dendrimer film was also confirmed by studying the electron-transfer-blocking properties of the film (see Supporting Information), which was revealed by studying the redox behavior of ferrocyanide anions and ruthenium hexamine cations on the modified electrode. The blocking of electron transfer for the ruthenium hexamine cations and the unblocking for the ferrocyanide anions showed the presence of dendrimers on the surface.[25] The presence of the dendrimer on the film was also verified by the Grazing

CHEMISTRY
AN ASIAN JOURNAL

angle IR spectrum of the dendrimer-modified film (see Supporting Information).

Figure 2a–d shows the SEM images of the samples of Au–Pt, Au–Pt/Au, and Au–Pt/Ru. From these images we can see the particulate nature of the films. In the case of Pt, the variation in particle size ranges from micrometers to nanometers. For Pt/Au, the particle size is more or less uniform and falls within the range of hundreds of nanometers. In the case of Pt/Ru, the particles are smaller still (5–10 nm), but they aggregate. Figure 2d shows clearly that nanoclusters of 5–10 nm in size aggregate in the case of Au–Pt/Ru films. The PAMAM dendrimer provides multidentate chelating points for the nucleation of metal atoms on the dendrimer-modified gold electrode. The films were found to be highly stable.

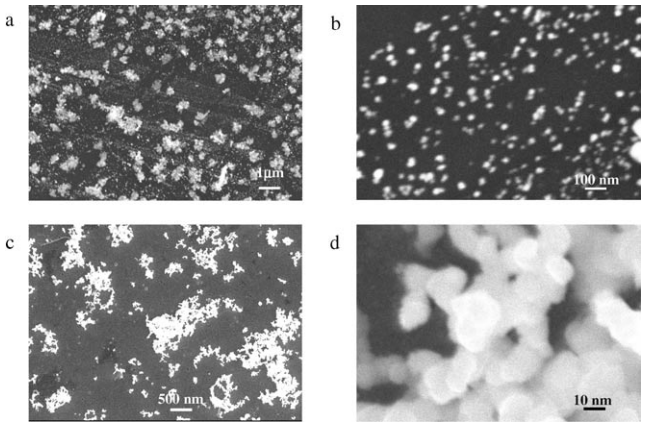

Figure 2. SEM images of a) Au–Pt, b) Au–Pt/Au, and c and d) Au–Pt/Ru films.

Figure 3a–c shows the topography and three-dimensional view of the dendrimer-trapped films Au–Pt, Au–Pt/Au, and Au–Pt/Ru, respectively. The images are similar to those of SEM. In the case of Au–Pt films, the particle size lies in the micrometer regime. The size of the cluster decreases for the Au–Pt/Au films. The Pt/Ru films consist of aggregated nanoclusters. One such cluster is shown in Figure 1c. Small clusters can also be seen nearby. The Au–Pt films (as seen from the three-dimensional view) are thicker than the Au–Pt/Au and Au–Pt/Ru films.

Figure 4 shows the XRD pattern of the Pt–dendrimer film on gold substrate. As the thickness of the films is in the nanometer range, the response due to the underlying gold surface was predominant in all cases. The Pt (111) peak expected at 39.77° is very feeble and insignificant, as it appeared at the foot of the strong Au (111) peak at 38.26°. The features of the underlying gold substrate is predominant in the XRD pattern because the film is very thin (nanometer range; see Figure 3). However, the presence of Pt can be identified by the presence of the peak at 81.28°, which corresponds to the Pt (311) plane. In the case of the Au–Pt/Au and Au–Pt/Ru films, the features of the underlying gold substrate are also predominant.

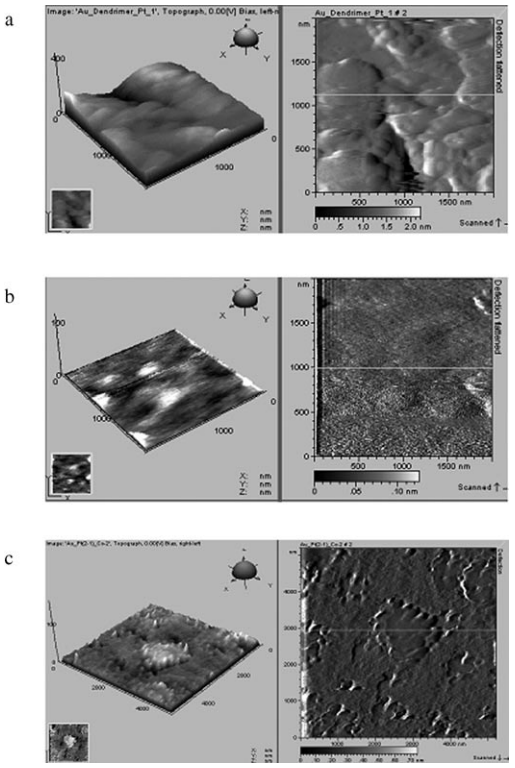

Figure 3. Topography (right) and three-dimensional view (left) of the films a) Au–Pt, b) Au–Pt/Au, and c) Au–Pt/Ru.

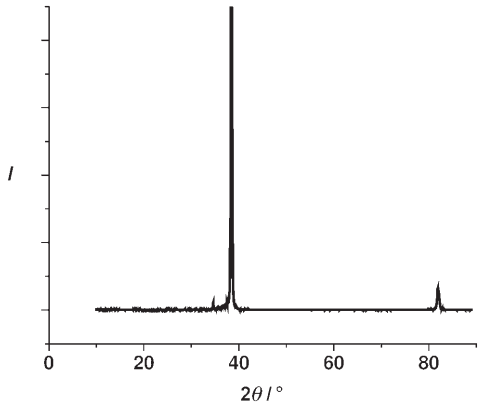

Figure 4. XRD pattern of the Au–Pt film.

Figure 5 shows the hydrogen-adsorption region for the Au–Pt electrode. The peaks that correspond to strong and weak adsorption are well-defined. Interestingly, the hydrogen-adsorption coverage on Au–Pt is quite high relative to that on a polycrystalline Pt electrode of the same geometric area, which points to the very high surface area of the dendrimer-derived Pt films. The multidentate nature of dendrimer molecules leads to a high loading of Pt in the dendrimer-derived films, and the particulate nature of the films increases the surface area. The hydrogen-adsorption charge was 1.25 $mC\,cm^{-2}$ and is very high relative to the monolayer charge of about 210 $\mu C\,cm^{-2}$, which is higher than that observed for polycrystalline bulk Pt electrodes.[26,27]

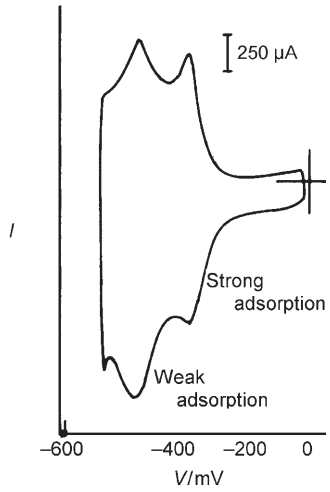

Figure 5. Cyclic voltammogram showing the hydrogen-adsorption region for the Au–Pt electrode at a scan rate of 50 mV s^{-1} in 0.5 M sulphuric acid.

The underpotential deposition of atomic hydrogen is a structure-sensitive catalytic process characteristic of the Pt surface. The hydrogen adsorption–desorption peaks occurred over a potential range similar to that for polycrystalline Pt. The anodic and cathodic potentials for weakly adsorbed hydrogen occurred at −485 and −500 mV, respectively. The peaks corresponding to strongly adsorbed hydrogen were observed at −345 mV (both anodic and cathodic). In the case of polycrystalline Pt, the adsorption and desorption peaks for both strong and weak adsorption appeared as mirror images.[26] However, on Au–Pt thin film, only weak adsorption/desorption peaks occurred at the same potential, whereas the strong adsorption/desorption peaks occurred with a minor potential difference of 15 mV. This is understood as being due to the nanostructured electrode surface. Notably, nanostructuring of the Pt electrode results[28] in a negative shift in the hydrogen-adsorption peak potentials relative to the bulk Pt electrode.

Figure 6 shows the cyclic voltammogram for methanol oxidation on the Au–Pt film in 0.5 M H_2SO_4. The methanol-oxidation peak occurred at a potential of 0.31 V, and the onset of oxidation occurred at −0.25 V. The oxide-assisted catalysis of methanol oxidation takes place at a higher potential. The oxidation potential in the reverse scan is also seen clearly in Figure 6 at 0.05 V. The hydrogen-adsorption region is not disturbed by methanol oxidation. This indicates that there are no substantial changes to the surface structure during this process. In the negative sweep, the current due to methanol oxidation nearly equalled that observed in the positive sweep. The modified electrode potential was held constant at the peak potential for methanol oxidation for nearly 10 min to check the effect of formation of products such as CO. After the controlled potential experiment, similar oxidation currents were observed for methanol oxidation, which indicates that blocking of catalytic sites by CO probably does not occur in this case. The values obtained

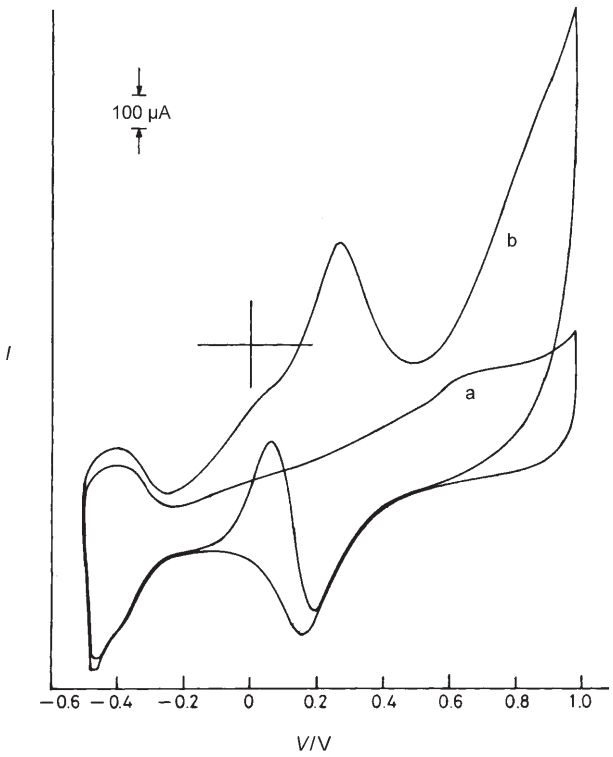

Figure 6. Cyclic votammogram showing a) background response for Au–Pt electrode and b) oxidation of methanol (0.034 M) at 50 mV s^{-1} in 0.5 M sulphuric acid.

herein are compared with the values for bulk Pt quoted in reference [29] (Table 1). The onset of oxidation occurred at a lower potential than for bulk Pt. However, the oxidation

Table 1. Electrocatalytic properties of the ultrathin metallic films for methanol oxidation.

Film	Methanol conc. [M]	Onset of oxidation potential [V]	Peak current density for oxidation [μA cm^{-2}]	Peak potential [V]	Reverse peak potential [V]
Pt	0.034	−0.25	1040	0.31	0.05
Pt/Au	0.034	−0.22	2800	0.28	−0.04
Pt/Ru	0.034	−0.24	7000	0.16	−0.17
Pt[29]	0.25	0.390 (−0.093)[a]	210	0.640 (0.16)*	–

[a] Values inside parentheses refer to potential with respect to Hg/Hg_2SO_4; values outside parentheses refer to potential with respect to Ag/AgCl.

peak potential occurred at a higher value than in the literature. The current values are nearly five times higher than that reported for bulk Pt even at the low concentration of 0.034 M (the concentration was nearly seven times lower than that reported for bulk Pt).

Figure 7 shows the cyclic voltammogram for methanol oxidation on Au–Pt/Au film. Methanol oxidation occurred at 0.28 V, and the onset of oxidation occurred at −0.20 V. The

CHEMISTRY
AN ASIAN JOURNAL

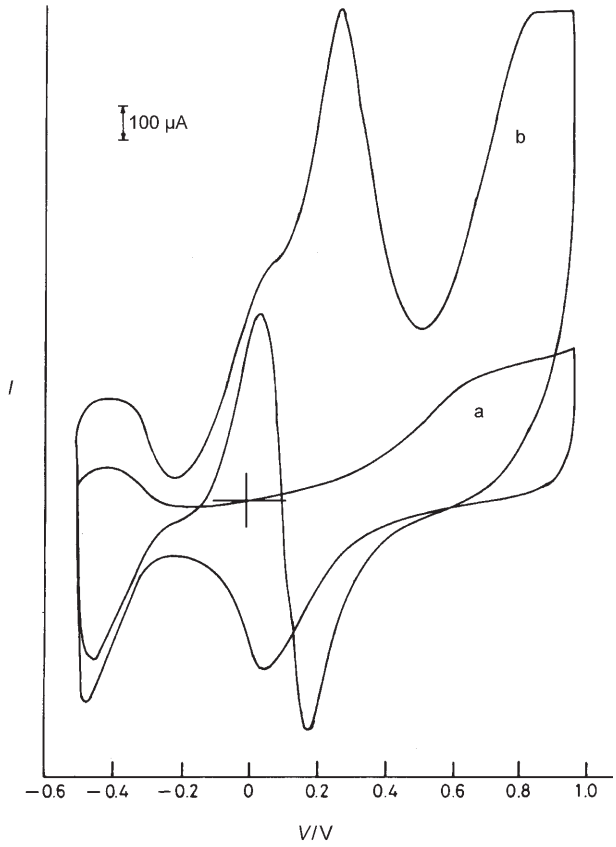

Figure 7. Cyclic votammogram showing a) background response for the Au–Pt/Au electrode and b) oxidation of methanol (0.034 M) at 50 mV s^{-1} in 0.5 M sulphuric acid.

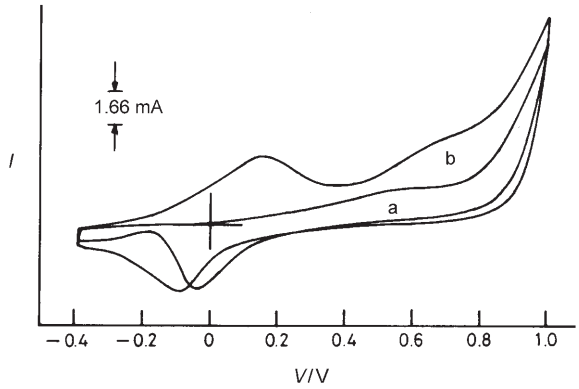

Figure 8. Cyclic votammogram showing a) background response for the Au–Pt/Ru electrode and b) oxidation of methanol (0.034 M) at 50 mV s^{-1} in 0.5 M sulphuric acid.

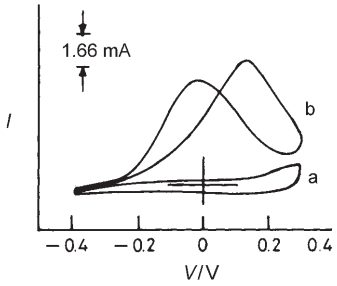

Figure 9. Cyclic votammogram showing a) background response for the Au–Pt/Ru electrode and b) oxidation of methanol (0.034 M) at 50 mV s^{-1} over a restricted potential range in 0.5 M sulphuric acid.

reverse oxidation took place at 0.04 V. The hydrogen-adsorption region remained intact in this case, which also indicates the absence of structural changes at the surface. The overpotential for methanol oxidation was decreased slightly (by 30 mV) compared to Au–Pt film. The catalytic currents were nearly 13 times higher than that observed for Au–Pt films (Table 1).

Figure 8 shows the cyclic voltammogram for methanol oxidation on Au–Pt/Ru film. In this case, methanol oxidation occurred at the lower potential of 0.16 V, and the onset of oxidation occurred at −0.24 V. The reverse oxidation took place at −0.17 V. The hydrogen-adsorption region is absent, thus indicating structural changes at the surface of the electrode. The catalytic currents were very high; they were 33 times that of Au–Pt film.

Figure 9 shows the methanol-oxidation cyclic voltammogram recorded within a restricted potential region. The currents due to methanol oxidation in the forward and reverse scans remained more or less the same, thus indicating a smooth unblocked surface. The oxidation behavior for Au–Pt/Au is similar to that for Au–Pt. The hydrogen-adsorption region remained intact during the electrooxidation of methanol. The current due to methanol oxidation during both positive and negative sweeps stayed the same. In the case of Au–Pt/Ru, the hydrogen-adsorption region is absent. Au is known to be a poor catalyst for the oxidation of hydrocarbons. In this work, the oxidation of hydrocarbons catalyzed by Au–Pt/Au films occurred at lower potential than with oxide-assisted catalysis. The potentials and current densities of methanol oxidation are given in Table 1. It is clear that Au–Pt/Ru films give rise to very large catalytic currents. Relative to literature reports[29] for similar reactions, the catalytic activity of our films were found be greater (Table 1). The literature values represent catalytic currents for high concentrations of methanol (0.25 M). The concentrations employed in our case were nearly seven times lower, but the catalytic currents were 33 times higher for the Au–Pt/Ru films. Here the peak potential for the oxidation of methanol nearly coincided with those of bulk Pt. However, in the case of the Au–Pt and Au–Pt/Au films, the observed current values were higher, the onset of oxidation occurred at a lower potential, and the peak potential for the oxidation of methanol was higher than for the bulk Pt electrode. This is probably due to the presence of dendrimer film on the electrode surface.

Figure 10a shows the chronoamperograms recorded for the three films. Chronoamperometry was employed to test the activity of these three electrodes further. The electrode potential was stepped to the oxidation potential of methanol in each case. For the Pt/Ru films, the steady-state current re-

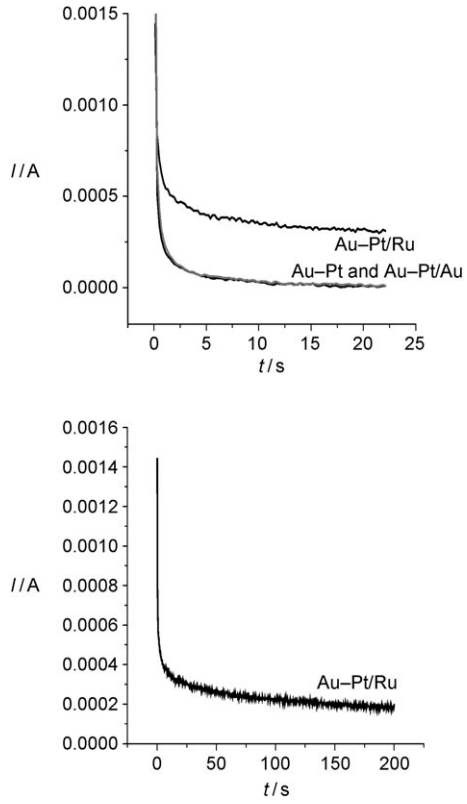

Figure 10. a) Chronoamperograms showing the variation of current with time at the methanol-oxidation potential for the Au–Pt, Au–Pt/Au, and Au–Pt/Ru electrodes. b) Chronoamperogram showing the variation of current with time at the methanol-oxidation potential for the Au–Pt/Ru electrode.

mained at a higher value than for the Au–Pt and Au–Pt/Au films. In the case of Au–Pt and Au–Pt/Au, the currents reached near-zero values within 13 s. However, for the Au–Pt/Ru films, a constant current of 0.2 mA was observed even after 200 s (Figure 10b). This shows that Au–Pt/Ru films should be better catalytic electrodes for practical applications.

Figure 11 shows the electrochemical impedance spectra recorded for the three films at the oxidation potential of methanol. The Nyquist plots reveal that the R_{ct} (charge-transfer resistance) value is significantly lower for the Pt/Ru films. In the case of the Au–Pt film, a very high R_{ct} value of nearly 11 000 Ω was obtained. For Au–Pt/Ru and Au–Pt/Au, the R_{ct} values are close to 1200 Ω. (The R_{ct} values were calculated by extrapolating the curve to a semicircle and then measuring its diameter.) This indicates facile charge transfer in the case of the bimetallic films.

Conclusions

The novel method proposed in this work with dendrimers as anchors for the preparation of Pt films resulted in very high catalytic activity. The surface area of the Pt film is very high

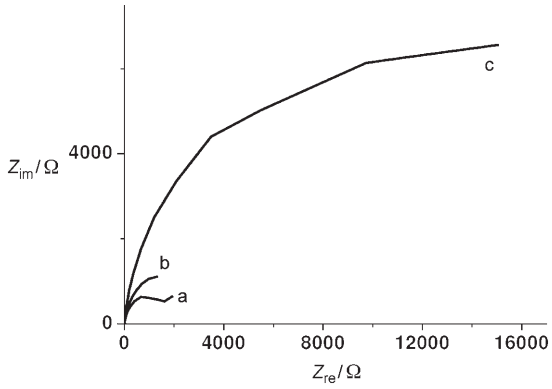

Figure 11. Impedance spectra for a) Au–Pt/Ru, b) Au–Pt/Au, and c) Au–Pt electrodes recorded at the oxidation potential of methanol.

as shown by hydrogen-adsorption studies. As dendrimers contain tens to hundreds of functional groups at the periphery, the aggregate strength of the multidentate interactions with the gold substrate leads to the formation of robust films. The numerous tertiary amine groups inside the dendrimer serve as nucleation points for the growth of these catalytic films. The films exhibit very high catalytic currents even at very low hydrocarbon concentrations. In the case of the Au–Pt/Ru films, the hydrogen-adsorption region was absent, which indicates structure variation at the surface. The structural effects will be addressed in future work. It was observed by chronoamperometry that currents were sustained for a longer period in the case of Au–Pt/Ru. The individual particles are 5–8 nm in size, and this may be the reason for the high catalytic activity of these films. Such catalytic films with large surface area and high catalytic currents are desirable for applications such as waste-water treatment and use in sensors and fuel cells. In this study, catalytically active thin films were formed on gold substrates, which are normally inert to hydrocarbon oxidation, with the help of dendrimers acting as anchors. The modification protocols described herein offer versatility and scope for the design of effective electrocatalysts, especially in the context of microfuel cells and "dendrichips". Materials of high surface-to-volume ratio that can be generated by using particles nucleated on anchor dendrimer matrices are more suitable than bulk polycrystalline Pt electrodes for miniaturized electrochemical systems, especially when platforms such as micrototal analytical systems are involved.

Experimental Section

Materials

$G4NH_2$ (Aldrich) and the reducing agent hydroxylamine hydrochloride (Ranbaxy) were used as received. Gold substrates (1000-Å gold coating on silicon wafers with an intermediate adhesion layer of 100-Å thick Ti, procured from Lance Goddard Associates, USA) of geometric area 0.5 cm^2 were used for platinum-film formation and as working electrodes for the electrooxidation of methanol.

Formation of Pt Thin Films on Gold Substrates

The gold substrates were cleaned by sonication in acetone followed by distilled water for 5 min each and then immersed in a solution of $G4NH_2$ (0.035 mM) in ethanol overnight. After 24 h, the substrates were removed and heated under reflux in the presence of hydroxylamine hydrochloride (1%) and K_2PtCl_4 (10 mM) for 5 h at 60 °C. The stability of the dendrimer-derived films was checked in the electrochemical cell containing the supporting electrolyte. The films deposited without the dendrimer, while patchy, were found to be unstable in the electrolyte solutions. The films were also prepared with Au or Ru in combination with Pt. The ratio of the concentration of Pt to Au or Ru was maintained at 2:1.

Electrochemical Characterization

Cyclic voltammograms were recorded by using a Wenking Potentioscan (POS 88) along with an *x–y/t* recorder (Rikadenki, Japan). Pt was used as the counterelectrode, and $Hg/Hg_2SO_4/H_2SO_4$ (0.5 M) (MSE) was used as the reference electrode. All electrochemical measurements were made with respect to the MSE. The experiments were carried out in 0.5 M H_2SO_4.

Impedance spectra were recorded over the frequency range 10 mHz–100 kHz with an AC amplitude of 10 mV in 0.5 M H_2SO_4, with the Au–Pt, Au–Pt/Au, and Au–Pt/Ru film electrodes at potentials corresponding to the oxidation of methanol in the forward scan, by using the advanced electrochemical system PARSTAT 2263. The applied potential for each electrode is given as follows: Au–Pt: 0.31 V; Au–Pt/Au: 0.28 V; Au–Pt/Ru: 0.26 V.

Chronoamperometric experiments were carried out by using PARSTAT 2263 at the methanol-oxidation potential with a Pt counterelectrode and an MSE reference electrode in 0.5 M H_2SO_4.

SEM images of the samples were recorded on a Hitachi Model S3000H scanning electron microscope. AFM images were obtained with a Molecular Imaging PicoSPM by using 30-nm gold-coated silicon nitride cantilevers (force constant 0.12 $N\,m^{-1}$). XRD patterns of the films were recorded (PANalytical, Model X'pertPRO) with a CuK source (maximum 2.2 kW).

Acknowledgements

We acknowledge the Department of Science and Technology, New Delhi, India and the Defence Research and Development Organisation, New Delhi, India for funding this work.

[1] R. M. Crooks, M. Zhao, L. Sun, V. Chechik, L. K. Yeung, *Acc. Chem. Res.* **2001**, *34*, 181–190.
[2] R. M. Crooks, B. I. Lemon, L. Sun, L. K. Yeung, M. Zhao, *Top. Curr. Chem.* **2001**, *212*, 81–135.
[3] R. M. Crooks, V. Chechik, B. I. Lemon, L. Sun, L. K. Yeung, M. Zhao in *Metal Nanoparticles* (Eds.: D. L. Feldheim, C. A. Fossji), Marcel Dekker, New York, pp. 261–296.
[4] R. W. J. Scott, O. M. Wilson, R. M. Crooks, *J. Phys. Chem. B* **2005**, *109*, 692–704.
[5] J. M. J. Frechet, D. A. Tomalia, *Dendrimers and Other Dentritic Polymers*, John Wiley & Sons, Chichester, **2001**.
[6] A. Bielinska, J. D. Eichman, I. Lee, J. Baker, Jr., R. L. Balogh, *J. Nanopart. Res.* **2002**, *4*, 395–403.
[7] K. Esumi, H. Houdatsu, T. Yoshimura, *Langmuir* **2004**, *20*, 2536–2538.
[8] S. Raghu, R. G. Nirmal, J. Mathiyarasu, S. Berchmans, K. L. N. Phani, V. Yegnaraman, *Catal. Lett.*, submitted.
[9] M. Zhao, L. Sun, R. M. Crooks, *J. Am. Chem. Soc.* **1998**, *120*, 4877–4878.
[10] Y. Li, M. A. El-Sayed, *J. Phys. Chem. B* **2001**, *105*, 8938.
[11] Y. Niu, L. K. Yeung, R. M. Crooks, *J. Am. Chem. Soc.* **2001**, *123*, 6840–6846.
[12] Y. Li, M. A. El-Sayed, *J. Phys. Chem. B* **2001**, *105*, 8938–8943.
[13] E. H. Rahim, F. S. Kamounah, J. Frederiksen, J. B. Christensen, *Nano Lett.* **2001**, *1*, 499–501.
[14] M. Ooe, M. Murata, T. Mizugaki, K. Ebitani, K. Kaneda, *Nano Lett.* **2002**, *2*, 999–1002.
[15] A. Manna, T. Imae, K. Aoi, M. Okada, T. Yogo, *Chem. Mater.* **2001**, *13*, 1674–1681.
[16] Y. M. Chung, H. K. Rhee, *Catal. Lett.* **2003**, *85*,159–164.
[17] N. Toshima, T. Yonezawa, K. Kushihashi, *J. Chem. Soc. Faraday Trans.* **1993**, *89*, 2537–2543.
[18] R. W. J. Scott, A. K. Datye, R. M. Crooks, *J. Am. Chem. Soc.* **2003**, *125*, 3708–3709.
[19] R. W. J. Scott, O. M. Wilson, S. K. Oh, E. A. Kenik, R. M. Crooks, *J. Am. Chem. Soc.* **2004**, *126*, 15583–15591.
[20] M. Zhao, R. M. Crooks, *Adv. Mater.* **1999**, *11*, 217.
[21] H. Ye, R. M. Crooks, *J. Am. Chem. Soc.* **2005**, *127*, 4930–4934.
[22] K. Esumi, S. Akiyama, T. Yoshimuna, *Langmuir* **2003**, *19*, 7679.
[23] T. Endo, T. Yoshimura, K. Esumi, *J. Colloid Interface Sci.* **2005**, *286*, 602.
[24] S. Raghu, S. Berchmans, K. L. N. Phani, V. Yegnaraman, *Pramana* **2005**, *65*, 821.
[25] S. Berchmans, M. Vergheese, A. L. Kavitha, M. Veerakumar, V. Yegnaraman, *J. Electroanal. Chem.*, submitted.
[26] A. J. Bard, L. R. Faulkner, *Electrochemical Methods, 2nd ed.*, John Wiley & Sons Inc., New York, **2001**, p. 560.
[27] J. Clavillier in *Electrochemical Surface Science: Molecular Phenomena at Electrode Surfaces* (Ed.: M. P. Soriaga), *ACS Symposium Series 378*, American Chemical Society, Washington D.C., **1988**, p. 202.
[28] M. Z. Markarian, M. El Harakeh, L. I. Halaoui, *J. Phys. Chem. B* **2005**, *109*, 11616–11621.
[29] E. Casado-Rivera, D. J. Volpe, L. Alden, C. Lend, C. Downie, T. Vazques-Alvares, A. C. D. Angelo, F. J. Disalvo, H. D. Abruna, *J. Am. Chem. Soc.* **2004**, *126*, 4043–4049.

Received: January 16, 2007
Published online: May 10, 2007

